

Sagnac effect in a fiber-optic interferometer

A. N. Gur'yanov, D. D. Gusovskii, G. G. Devyatykh, E. M. Dianov, A. Ya. Karasik, V. A. Kozlov, V. B. Neustruev, and A. M. Prokhorov
P. N. Lebedev Physics Institute, USSR Academy of Sciences

(Submitted 19 June 1980)

Pis'ma Zh. Eksp. Teor. Fiz. **32**, No. 3, 240–243 (5 August 1980)

A ring interferometer, which uses a 285-m-long, single-mode, fiber lightguide and is capable of measuring angular rotation velocities down to 0.3 deg/sec, was built.

PACS numbers: 42.80.Mv, 07.60.Ly

The development of low-loss glass fiber lightguides (GFL) has made it possible to look at the Sagnac effect in a fiber-optic interferometer from a new point of view and to evaluate its capabilities for making gyroscopes.^{1,2} As is known (see, for example, Ref. 3), the Sagnac effect can be described as follows: when a ring interferometer rotates with an angular velocity ω , a displacement ΔZ of the interference fringes is observed:

$$\Delta Z = \frac{4 \omega S}{\lambda_0' c}, \quad (1)$$

where S is the area covered by the light rays, and λ_0' and c are the light wavelength and velocity in a vacuum (the rotation axis is perpendicular to the interferometer plane). The use of GFL makes it possible to increase the number of circuits of a given perimeter by the light rays and to greatly broaden the capabilities of the interferometer for detecting small ω . In the case of a GFL wound on a spool of radius R , Eq. (1) is written in the form

$$\Delta Z = \frac{4 \cdot \omega S N}{\lambda_0' c} = \frac{2 \omega L R}{\lambda_0' c}, \quad (2)$$

where N is the number of turns and L is the GFL length.

Figure 1 shows the experimental setup. The light from a laser (L) strikes the beamsplitter plate (BP); then the light beams of equal intensity pass through the lenses (O) and enter the ends of the GFL, wound on a spool (S) with $R = 25$ cm. The two light beams, which circulate in the GFL in opposite directions, come together at the beamsplitter plate, forming an interference pattern in the plane of the photodetector (PD). Because of the flexibility of the GFL ends, we were able to rotate only the spool within the limits of a 180° sector; the GFL ends remained stationary from the point where the radiation entered them to the center of the spool. The shearing of the interference fringes during rotation of the coil was recorded from the relative variation of the intensity at a point on the interference pattern selected by using the diaphragm (D). A polarizer (P), which was used to eliminate the unwanted, linearly polarized laser radiation reflected from the lenses, was placed in front of the photodetector. To record

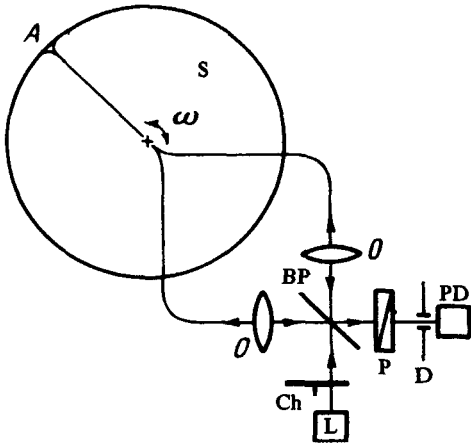


FIG. 1. Schematic of the experimental apparatus.

the ΔZ , we modulated the laser radiation by the chopper (Ch) and used a synchronous, signal-detection circuit. The radiation source was a He-Ne laser with $\lambda = 0.63 \mu\text{m}$ and radiation power $\sim 8 \text{ mW}$.

In our experiments we used two types of GFL with an $\text{SiO}_2 + \text{GeO}_2$ core⁴: the first had a length $L = 285 \text{ m}$ and a core diameter $\phi = 5.6 \mu\text{m}$, the second had $L = 770 \text{ m}$ and $\phi = 7 \mu\text{m}$. In both GFL the difference in the refractive indices of the core and the sheath was $\Delta n = 2.4 \times 10^{-3}$ and the refractive index of the core was $n = 1.461$. For $\lambda = 0.63 \mu\text{m}$ the first GFL was single-mode, while the second was two-mode, and the losses were $\sim 32 \text{ dB/km}$ in both GFL as a result of transmission at this wavelength.

To obtain an interference pattern, the GFL ends were placed at different distances relative to the foci of the lenses; this resulted in different curvature of the wavefronts of the two interfering light beams. The densitometric trace of the photographed interference pattern for a single-mode GFL is shown in the upper part of Fig. 2a ($\omega = 0$), which also shows the transformation of this interference pattern when the spool rotates at $\omega = \pm 18 \text{ deg/sec}$ (the “+” and “-” signs represent the spool rotation in the opposite direction). We can see that the interference ring fringes are sheared as a result of the spool rotation; the shearing in this case depends on the rotation direction. By introducing the laser radiation into one of the GFL ends at some angle, we obtained an interference pattern (Fig. 2b, $\omega = 0$) which greatly differs from that in Fig. 2a. The central bright spot appears dark, which indicates that there is an additional phase shift between the circulating light beams. As will be shown below, the introduction of an artificial phase shift is important for recording small ω . A variation of ω produces a strong shearing of the fringes, and the dark central spot becomes a bright spot as ω is increased to 18 deg/sec .

Figure 3 shows a variation of the intensity (ΔI) of the central spot of the interference pattern as a function of ω for the single-mode GFL. The interferometer adjustment and recording conditions were chosen in such a way that a linear dependence could be obtained for small ω . The difference between the ω values for the maximum

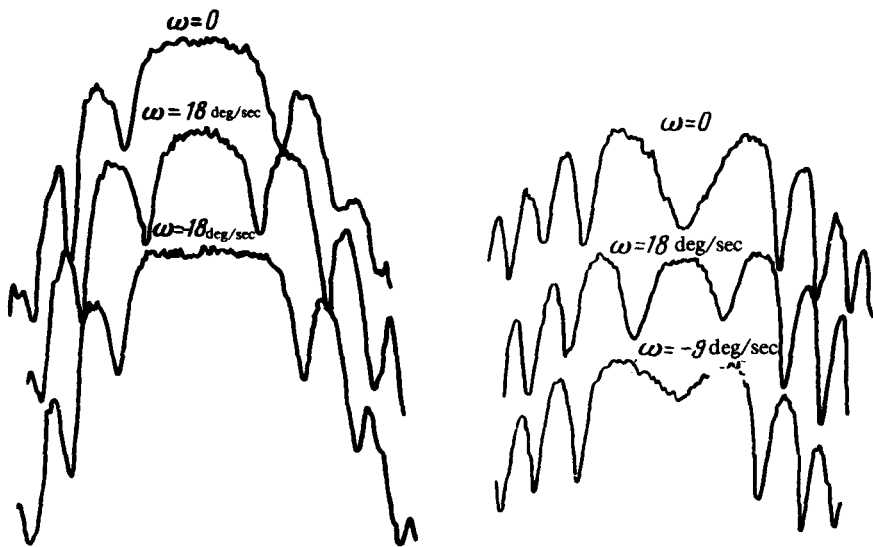


FIG. 2. Interference pattern produced as a result of rotation at different angular velocities.

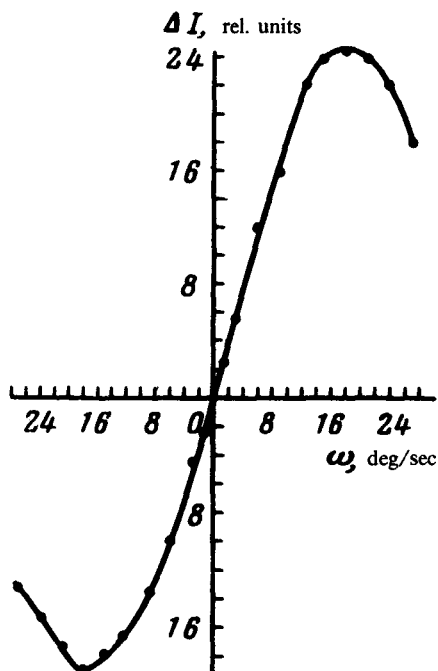


FIG. 3. Dependence of relative change in the intensity of the interference fringe on the angular rotation velocity.

and minimum of the ΔI dependence corresponds to a displacement of one-half an interference fringe. We obtained a single-mode GFL the values $\omega = 74\text{--}76$ deg/sec from all the experiments for a one-fringe displacement. After substituting the initial data and the values of 76 and 74 deg/sec in Eq. (2), we obtained $\Delta Z = 1$ and 0.97, respectively. The minimum ω , which was measured for a single-to-noise ratio of 2, was 0.3 deg/sec, consistent with $\Delta Z = 4 \times 10^{-3}$.

Experiments similar to ours have been performed earlier.^{2,5} It was shown² that ΔZ is a function of the refractive index and of dispersion of the GFL material,³ whereas Eq. (2) was verified elsewhere.⁵ Our measurements showed with sufficient accuracy that ΔZ does not depend on the properties of the GFL material.

A dependence similar to that in Fig. 3 was obtained by us for a two-mode GFL. However, the accuracy in determining for it was poorer than for a single-mode GFL. Despite the fact that both colliding rays propagated in the same GFL, slight external temperature fluctuations redistributed the intensity in the interference pattern, whereas such effect was not observed in a single-mode GFL.

According to the estimates of Ref. 6, the maximum sensitivity of the fiber-optic interferometer is $\sim 10^{-7}$ deg/sec. In practical terms, this requires an increase in the GFL length and hence a shift of λ toward the near IR region, where the GFL has low light-transmission losses,⁷ and also the use of more elaborate recording circuits.

¹V. Vali and R. W. Shorthill, *Appl. Opt.* **15**, 1099 (1976).

²V. Vali, R. W. Shorthill, and M. F. Berg, *Appl. Opt.* **16**, 2605 (1977).

³E. J. Post, *Rev. Mod. Phys.* **39**, 175 (1967).

⁴A. N. Gur'yanov, D. D. Gusovskii, G. G. Devyatykh, E. M. Dianov, M. M. Mirakyan, V. B. Neustruev, A. V. Nikolaichik, A. M. Prokhorov, and V. F. Khopin, *Kvantovaya Elektron.* **7**, No. 8 (1980) [*Sov. J. Quantum Electron.* (in press)].

⁵E. R. Leeb, G. Schiffner, and E. Schreiterer, *Appl. Opt.* **18**, 1293 (1979).

⁶S. -C. Lin and T. Giallorenzi, *Appl. Opt.* **18**, 915 (1979).

⁷E. M. Dianov, *Kvantovaya Elektron.* **7**, 453 (1980) [*Sov. J. Quantum Electron.* **10**, 259 (1980)].